Simple dynamical models for hierarchical bunching

Hidetsugu Sakaguchi and Norio Fujimoto
Department of Applied Science for Electronics and Materials, Interdisciplinary Graduate School of Engineering Sciences, Kyushu University, Kasuga, Fukuoka 816-8580, Japan
(Received 28 April 2003; published 3 November 2003)

Simple one-dimensional models for hierarchical bunching are proposed. A uniform state with equal spacing is linearly unstable and bunching clusters are created. The bunching clusters are further merged into even larger clusters. The coarsening process towards the larger clusters obeys a power law for the long-range forces. The exponent of the power law depends on the long-range forces. A continuum version of the lattice model with linear repulsive force is studied more in detail. The model has a form of a kind of spinodal decomposition. The coarsening dynamics is similar to a one-dimensional version of the Ostwald ripening.

DOI: 10.1103/PhysRevE.68.056103 PACS number(s): 05.70.Fh, 89.75.Kd, 64.60.−i

I. INTRODUCTION

Bunching phenomena are observed in various research fields. Microwave oscillation is induced by the bunching of the electron density and the electric field in the Gunn effect for GaAs [1]. Traffic congestion is a bunching phenomenon of car flow [2,3]. Step bunching was observed on the vicinal surfaces of Si(111) [4,5]. Step bunching which exhibits the power-law growth was found in several experiments [6]. The hierarchical step bunching on the vicinal surfaces was studied theoretically based on several model equations [7,8].

The bunching phenomena are explicitly shown by numerical simulation of dynamical equations for the positions of bunching objects. Bando *et al.* proposed an equation of motion for the position of each vehicle for the problem of traffic congestion [9]. For the problem of the step bunching, explicit dynamical equations of motion for the position of each step were derived based on the diffusion equation and the boundary conditions for adatoms by several authors [10], however, they have rather complicated forms to understand the bunching phenomena qualitatively. We propose an abstract but much simpler model equation to understand the essence of bunching phenomena, and study the time evolution of hierarchical bunching with numerical simulations and theoretical analyses.

II. SIMPLE DYNAMICAL MODELS FOR HIERARCHICAL BUNCHING

We consider a one-dimensional system of N elements. The model equation is written as

$$\frac{dy_i}{dt} = -f(y_{i+1}-y_i)+f(y_i-y_{i-1}), \tag{1}$$

where y_i is the position of the ith element, satisfying $y_1 < y_2 < \cdots < y_N$, and $f(l)$ is the force between the nearest neighbors, which depends only on the distance l between them. If the differential term on the left-hand side is replaced with the second differential term d^2y_i/dt^2, the equation becomes a model for lattice vibration. Our model is a lattice model and represents a dissipative and variational dynamics. There exists a potential function $\Sigma_i U(y_{i+1}-y_i)$, where $f(l)=-\partial U/\partial l$ for the dynamics and the potential decreases in time. We can assume various types of interactions between the neighboring elements. Similar to the interatomic force, we assume a short-range repulsive force expressed by a power law such as $f(l)=a/l^{\alpha}$ $(a>0)$ when l is sufficiently small. We use in this paper a repulsive force with exponent $\alpha=3$. The repulsive interaction with exponent $\alpha=3$ originates from the elastic energy in the problem of the step dynamics on vicinal surfaces. The short-range repulsive forces prevent the spacing between the nearest neighbors from being zero. We assume further several types of long-range interactions. For interatomic forces, the interaction becomes attractive in the long range in most cases. We can assume a model in which the long-range attractive force is expressed as $f=f_1(l)=-b/l^2$ $(b>0)$. The attractive force expresses a force like the Coulomb force between ions with opposite charges. We will study three other repulsive forces. The simplest one is a linear force $f=f_2(l)=bl$. We will study this model most in detail, since the model equation is the simplest and the hierarchical bunching appears most clearly. Two other simple repulsive forces are $f_3(l)=b\log l$ and $f_4(l)=b\tanh l$. Since Eq. (1) is invariant for the transform: $f(l)\to f(l)+c_0$, where c_0 is a constant, the model with the fourth repulsive force $f_4(l)$ is equivalent to a model with the force $f_4(l)-b=-2b\exp(-l)/[\exp(l)+\exp(-l)]$. The force $f_4(l)-b$ expresses an attractive force which decays exponentially for large l. Such exponentially damping force is often assumed as an interatomic force. The exponentially damping force and the Coulomb-type forces may be plausible forces in actual physical systems. The model with the linear force may be obtained through some linearization of realistic systems. The hierarchical bunching by the logarithmic force exhibits the power-law growth with the same exponent as the experiment for the step bunching as shown below.

A stationary solution to Eq. (1) is a uniform state with constant spacing $y_{i+1}-y_i=l_0$ for every i. The linearized equation for the perturbation δy_i from the stationary solution is expressed as

$$\frac{d\delta y_i}{dt} = f'(l_0)(-\delta y_{i+1}+2\delta y_i-\delta y_{i-1}). \tag{2}$$

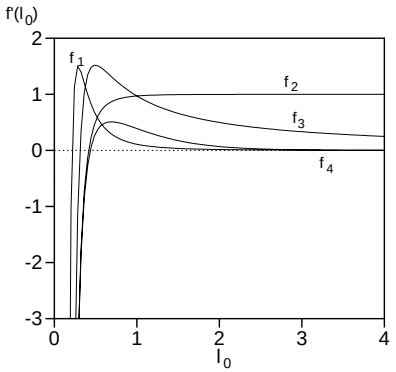

FIG. 1. Growth parameter $f'(l_0)$ for four kinds of functions $f=f_1(l)=-0.07/l^2+a/l^3$, $f=f_2(l)=l+a/l^3$, $f_3(l)=\log l+a/l^3$, and $f_4(l)=\tanh l+a/l^3$ at $a=0.01$.

The linear growth rate λ_k for the Fourier amplitude $\delta y_k=\Sigma_{j=1}^{N}\delta y_j e^{-ikj}$ with wave number k is calculated as $\lambda_k=(2-2\cos k)f'(l_0)$. If $f'(l_0)$ is positive, the linear growth rates are all positive for any wave numbers, and the uniformly spacing state is unstable. Especially the linear growth rate is maximum at $k=\pi$, which corresponds to the alternating mode $\delta y_i\sim(-1)^i$. Figure 1 displays the function $f'(l_0)$ for the four repulsive forces $f_1(l)=0.01/l^3-0.07/l^2$, $f_2(l)=0.01/l^3+l$, $f_3(l)=0.01/l^3+\log l$, and $f_4(l)=0.01/l^3+\tanh l$. The uniform states with sufficiently small l_0 are stable for all models, owing to the short-range repulsive force. For $f=f_1(l),f_2(l)$ and $f=f_3(l)$, the uniform states are always unstable for large l_0 satisfying $l_0>0.214$ for $f=f_1(l)$, $l_0>0.416$ for $f=f_2(l)$ and $l_0>0.311$ for $f=f_3(l)$, because of the long-range repulsive force. For $f=f_4(l)=\tanh l+a/l^3$, $f'(l_0)$ takes positive values in an intermediate range of l_0, but it becomes sufficiently small but negative for large l_0. It is because the derivative of $\tanh l$ decays to zero exponentially, but that of a/l^3 decays in a power law. The instability occurs only in an intermediate range of l_0. This type of instability occurs in model equations studied in Refs. [9] and [10].

We have performed numerical simulations to study the time evolution of the unstable states using the Runge-Kutta method with time step 0.000 05. The initial spacing is $l_0=0.7$. Figure 1 is a time evolution of Eq. (1). The periodic boundary conditions $y_{N+1}=y_1+L$ and $y_0=y_N-L$ are used for numerical simulations. The total number of elements is $N=100$ and the system size $L=Nl_0$ is equal to 70. The initial position is $y_i=0.7i+r$, where r is a random number between 0 and 0.0001. Figure 2 displays time evolutions of $\{y_i\}$ for four kinds of forces. Since the uniform state is unstable, the bunching occurs for all four kinds of forces.

Since the linear growth rate is maximum for the alternating mode, pairing of neighboring elements tend to occur first. It is the minimum bunching cluster. The uniform configuration constructed by the pair clusters is also unstable and the clustering proceeds further. Many merging processes of the bunched clusters are seen in Fig. 2. Qualitatively similar type time evolutions are observed for different initial conditions, although the detailed bunching processes are different for different initial conditions. Figure 2(a) is a time evolution for

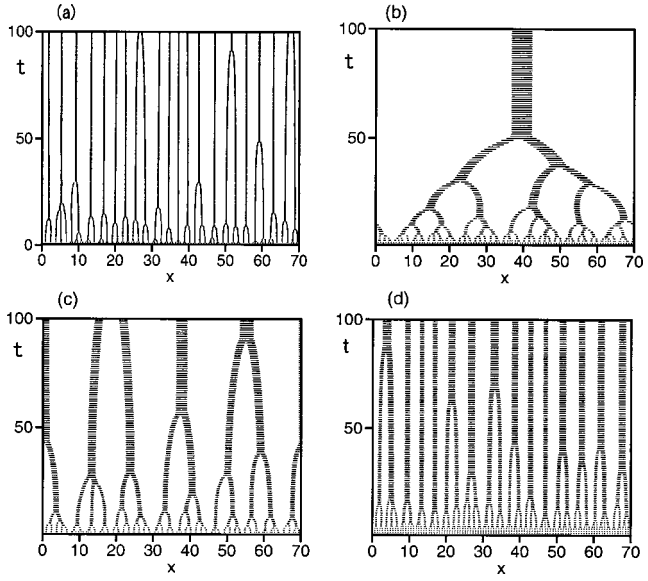

FIG. 2. Time evolutions of $\{y_i\}$ for (a) $f=f_1(l)=-0.3/l^2+a/l^3$, (b) $f=f_2(l)=l+a/l^3$, (c) $f=f_3(l)=\log l+a/l^3$, and (d) $f=f_4(l)=\tanh l+1/l^3$ at $a=0.01$.

$f=f_1(l)=0.01/l^3-0.3/l^2$, and Fig. 2(b) is a time evolution for $f=f_2(l)=0.01/l^3+l$. The merging of bunched clusters occurs hierarchically and only one large cluster survives after $t\sim51$. We have performed similar simulations starting from 200 different initial conditions where the random numbers in $y_i=0.7i+r$ are different, and calculated the final coalescence time, when only one large cluster is obtained. The average value of the final coalescence time was 60.5 and the variance was 12. The final coalescence time and the time evolution of the clustering depends on the small difference of the initial positions, since the initial state is linearly unstable, but only one large cluster is obtained in similar times. For $f=f_3(l)=0.01/l^3+\log l$, similar hierarchical bunchings occur, but the time evolution is slower than the case of $f=f_2(l)$. We have performed a longer simulation for the same initial condition and found that the single large cluster was obtained at $t\sim1270$. It takes much longer time to get the single cluster for $f=f_3(l)$ than $f=f_2(l)$. For $f=f_4(l)=0.01/l^3+\tanh l$, the time evolution of cluster bunching becomes very slow, bunched clusters are located with nearly equal spacing at $t=100$. The hierarchical bunching is considered to be due to long-range repulsive force.

We have calculated the time evolution of the average value $\langle l_b(t)\rangle$ of the distances between the bunched clusters in larger-size simulations. The spacings $l=x_{i+1}-x_i$ between neighboring elements inside the bunched clusters are sufficiently smaller than the spacings $l=x_{i+1}-x_i$, where the ith and $i+1$th elements belong to different clusters. We have judged a spacing l between neighboring elements as the distance between the bunched clusters, when the spacing is larger than a critical value such as the initial spacing 0.7. Then, $\langle l_b\rangle$ was evaluated as the average value of the spacing which is larger than the critical value. The average value $\langle l_b(t)\rangle$ hardly depends on the critical value. In this simulation, the total number N is 3000, and the ensemble average was taken for 20 different initial conditions, where the ran-

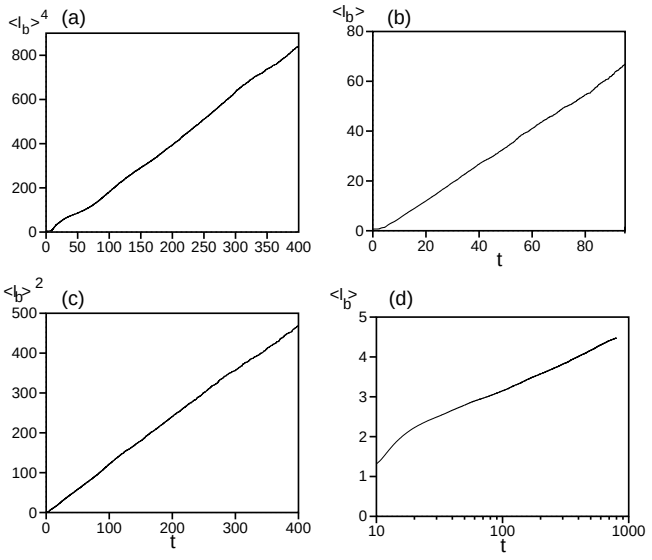

FIG. 3. (a) Time evolutions of the average size $\langle l_b(t)\rangle^4$ of the distances between the bunched clusters for $f=f_1(l)=-0.3/l^2+0.01/l^3$. (b) Time evolutions of the average size $\langle l_b(t)\rangle$ of the distances between the bunched clusters for $f=f_2(l)=l+0.01/l^3$. (c) Time evolution of $\langle l_b(t)\rangle\rangle^2$ for $f=f_3(l)=\log l+0.01/l^3$. (d) Time evolution of $\langle l_b(t)\rangle\rangle$ for $f=f_4(l)=\tanh l+0.01/l^3$. The time axis is plotted in a logarithmic scale.

dom numbers $\{r\}$ in the initial conditions are different. Figure 3(a) displays a time evolution of $\langle l_b(t)\rangle^4$ for $f=f_1(l)$. A linear growth for relatively large t implies that $\langle l_b(t)\rangle \sim t^{1/4}$. Figure 3(b) displays a time evolution of $\langle l_b(t)\rangle$ for $f=f_2(l)$. A linear growth is seen for relatively large t. The linear growth law implies that the hierarchical bunching proceeds fast as seen in Fig. 2(b). When the average spacing increases up to the order of system size L, the single large cluster is obtained. The linear growth of $\langle l_b(t)\rangle$ implies that the time necessary for the generation of the single large cluster is proportional to L. We have also calculated a time evolution of $\langle[\Delta l_b(t)]^2\rangle^{1/2}$, where $\Delta l_b(t)=l_b(t)-\langle l_b(t)\rangle$. The root-mean-square of the spacing between the bunched clusters increases also in proportion to t. Figure 3(c) displays a time evolution of $\langle l_b(t)\rangle^2$ for $f=f_3(l)$. The linear growth law implies that $\langle l_b\rangle \sim t^{1/2}$. This type of growth law with exponent 1/2 was observed in the experiment of the step bunching of vicinal surfaces [6]. From the linear growth of $\langle l_b(t)\rangle^2$, the time necessary for the generation of the single large cluster is expected to be proportional to L^2. It is consistent that the final coalescence times were 51 for $f=f_2(l)$ and 1270 for $f=f_3(l)$ in the simulations shown in Fig. 2. We have checked that the root-mean-square of the spacing between the bunched clusters increases also in a power law with exponent 1/2. Figure 3(d) displays a time evolution of $\langle l_b(t)\rangle$ for $f=f_4(l)=\tanh l+a/l^3$. The horizontal axis is plotted with a logarithmic scale. It implies that the average distance between the bunched clusters grows as $\langle l_b\rangle \sim \log t$, and the clustering of the bunched clusters is very slow as shown in Fig. 2(d).

The growth of the hierarchical bunching obeys a power law and the exponent depends on the power α of the long-range force $f(l)\sim l^\alpha$. We have not found such a power law for $f=f_4(l)=\tanh l+a/l^3$, since the repulsive force saturates exponentially. The exponent of the power-law growth is evaluated with a simple scaling method as follows. If the hierarchical bunching evolves uniformly and bunched clusters of number $n(t)$ appear at time t, the distance between the neighboring bunched clusters is estimated as $l_b(t)=L/n(t)$, and the number N_b of elements in each cluster is estimated as $N_b=N/n(t)$. If the summation of Eq. (1) is taken with respect to all the element i inside of each cluster, an equation for the averaged position $Y_j=\Sigma_i y_i/N_b$ of the jth bunched cluster is approximately obtained as

$$N_b\frac{dY_i}{dt}=-f(Y_{j+1}-Y_j)+f(Y_{j-1}-Y_j). \tag{3}$$

If the long-range force is approximated as $f(l)\sim l^\alpha$, the average distance between the neighboring clusters $l_b\sim Y_{j+1}-Y_j$ obeys the equation

$$N_b\frac{dl_b}{dt}\propto l_b\frac{dl_b}{dt}\sim l_b^\alpha. \tag{4}$$

Therefore, the time evolution of $l_b(t)$ is evaluated as $l_b(t)=t^{1/(2-\alpha)}$. The exponent for $\alpha=1$ $[f=f_2(l)]$ is 1, the exponent for $\alpha=0$ [including logarithmic law $f=f_3(l)$] is 1/2, and the exponent for $\alpha=-2$ $[f=f_1(l)]$ is 1/4. These results are consistent with the direct numerical simulations.

III. CONTINUUM EQUATION FOR HIERARCHICAL BUNCHING

The spacing of neighboring elements inside of the bunched cluster is very small but the interval between the neighboring bunched clusters is fairly large as shown in Fig. 2. The spacing between the neighboring elements changes discontinuously at the edge sites of the bunched clusters. In many bunching models such as car-following models and step bunching models, the spacing changes more continuously. If a next-nearest interaction is introduced as

$$\frac{dy_i}{dt}=-f(y_{i+1}-y_i)+f(y_i-y_{i-1}) -D(y_{i+2}-4y_{i+1}+6y_i-4y_{i-1}+y_{i-2}), \tag{5}$$

D is a coupling constant, the spacing changes more continuously. Figure 4 displays a time evolution of Eq. (5) with $f=f_2(l)=l+0.01/l^3$ and $D=1$. Hierarchical bunching occurs similarly to the case of $D=0$. But several elements locate between the bunched clusters, which makes the profile of spacing more smooth. The equation of motion for the spacing $l_i=y_{i+1}-y_i$ obeys

$$\frac{dl_i}{dt}=-f(l_{i+1})+2f(l_i)-f(l_{i-1}) -D(l_{i+2}-4l_{i+1}+6l_i-4l_{i-1}+l_{i-2}). \tag{6}$$

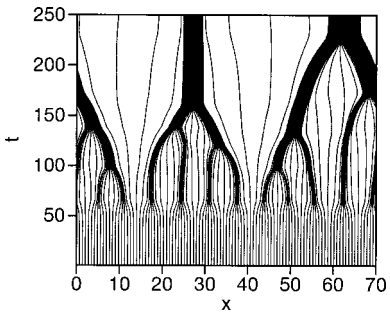

FIG. 4. Time evolution of $\{y_i\}$ for Eq. (5) for $f=l+0.01/l^3$ and $D=1$.

If we take a continuum approximation $l_i=l(x)$, Eq. (6) yields

$$\frac{\partial l}{\partial t}=-\frac{\partial^2}{\partial x^2}\left(-\frac{\partial U(l)}{\partial l}+D\frac{\partial^2 l}{\partial x^2}\right), \tag{7}$$

where $U(l)$ is a potential function satisfyng $-\partial U/\partial l=f(l)$. Equation (7) takes the same form as a model of spinodal decomposition in which the order parameter is conserved [11]. In the usual model of the spinodal decomposition, a bistable potential such as $U(l)=-(1/2)l^2+(1/4)l^4$ is assumed. The model equation is called the time dependent Ginzburg-Landau equation for the conserved order parameter. In our model of bunching, $U(l)$ is not a bistable function, for example, it is a monotonically decreasing function such as $U(l)=-(1/2)l^2+(a/2)l^{-2}$ for $f=f_2(l)=l+a/l^3$. Time evolution is therefore rather different from the usual Ginzburg-Landau equation for the conserved order parameter. We study the time evolution of the continuum model (7) for $f=f_2(l)=l+a/l^3$ for the sake of simplicity. Numerical simulation was performed with the pseudospectral method with 1024 modes with time step 0.0001. The system size $L=400$. Figure 5(a) displays a time evolution of $l(x,t)$ at $a=0.01$ and $D=1$. The initial condition is almost uniform $l(x)=0.7$. The uniform state is linearly unstable, and fluctuations with wave numbers $k\sim 1/\sqrt{2}$ grow fast, since the linear growth rate for larger wave number becomes negative by the term $-D\partial^4 l(x)/\partial x^4$ in contrast to the discrete model (1). Many small pulses appear from the wavy fluctuations.

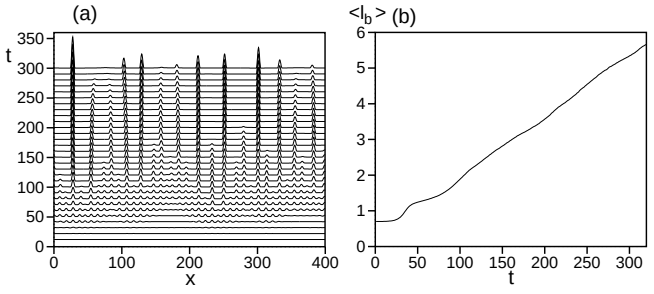

FIG. 5. (a) Time evolution of $l(x,t)$ for the continuum model (7) with $-\partial U/\partial l=l+0.01/l^3$ and $D=1$. (b) Time evolution of the average height of the survived pulses. We have calculated the quantity as the average of $l(x,t)$ satisfying $l(x)>0.7$.

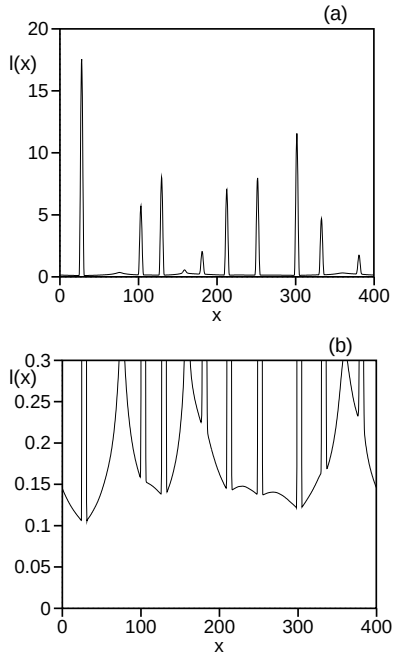

FIG. 6. (a) Profile of $l(x)$ at $t=300$. (b) Enlargement of (a) in the bottom region $0<l(x)<0.3$.

Then, competition among the pulses is observed. Small pulses decay and larger pulses grow further. The positions of very large pulses are almost stationary. The pulse number decreases in time, and the average height of the survived pulses increases. The large pulse corresponds to the large interval between the bunched clusters in the discrete model (1) or (5). The time evolution shown in Fig. 5(a) corresponds to the hierarchical bunching of the discrete model. Figure 5(b) displays the time evolution of the average height of the survived pulses. The numerical simulation was performed with a larger system of $L=1600$, and the ensemble average was taken for 20 different initial conditions. The average height increases in proportion to t. It is the same result as the discrete model as shown in Fig. 3(b). Figure 6(a) displays a profile of $l(x)$ at the final time of Fig. 5. Each pulse has different height, but the width is almost the same. Figure 6(b) is an enlargement of $l(x)$ in the bottom region $0<l(x)<0.3$. It is a feature that $l(x)$ takes smaller values around larger pulses than smaller pulses in the bottom region. These features of pulses are closely related to a family of stationary pulse solutions of Eq. (7).

A stationary solution of Eq. (7) satisfies generally $d^2\{f[l(x)]+Dd^2l(x)/dx^2\}/dx^2=0$. The integration of this equation yields $f[l(x)]+Dd^2l/dx^2=c+dx$, where c and d are integral constants. However, the stationary solutions for nonzero d correspond to steadily propagating solutions for the continuum approximation of Eq. (6), i.e., $dy_i/dt=$const. A relevant stationary solution corresponding to $dy_i/dt=0$ therefore satisfies

$$f[l(x)]+D\frac{d^2l}{dx^2}=c. \tag{8}$$

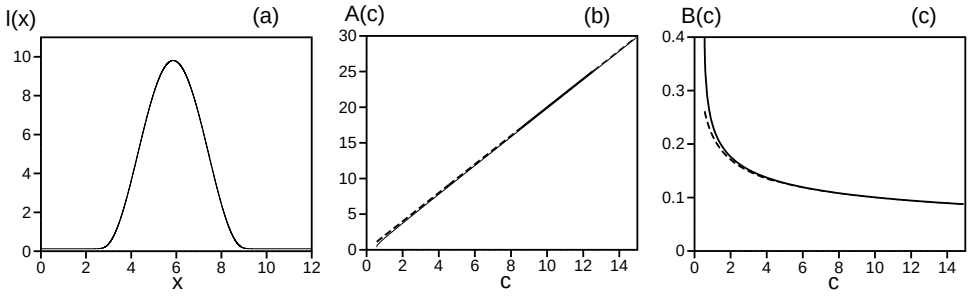

FIG. 7. (a) Pulse solution of Eq. (8) for $c=5$ and $D=1$. (b) Comparison of the numerically obtained pulse height $A(c)$ (solid curve) with the theoretical value $A(c)=2c$ (dashed curve). (c) Comparison of the numerically obtained bottom value $B(c)$ (solid curve) with the theoretical value $B(c)=(a/c)^{1/3}$ (dashed curve) with $a=0.01$.

Equation (8) has a form of Newton's equation in a potential $U'=-U(l)-c\cdot l=(1/2)l^2-(a/2)l^{-2}-c\cdot l$. The pulse solution is a homoclinic solution of Eq. (8). The pulse solution exists for $c>(3^{1/4}+3^{-3/4})a^{1/4}$. Figure 7(a) is an example of the stationary pulse solution by Eq. (8) for $c=5$. As c is increased, the pulse height increases. For sufficiently large l, the term a/l^3 can be neglected in Eq. (8). Then, Eq. (8) has a simple form: $d^2l/dx^2=(c-l)/D$. The pulse solution can be approximated at $l(x)=c+c\,\sin(x./\sqrt{D})$. As c is increased, the peak height of the pulse increases as $2c$, but the pulse width hardly depends on c. Figure 7(b) compares the peak height numerically obtained using Eq. (8) with the theoretical estimate $2c$. The difference is almost invisible. We can neglect the linear term l in Eq. (8) in the tail region. Then, Eq. (8) is simplified as $Dd^2l/dx^2=-a/l^3+c$. In the tail region of the pulse, $d^2l/dx^2=0$, therefore the bottom value of the pulse solution is evaluated as $l\sim(a/c)^{1/3}$. Figure 7(c) compares the bottom value obtained numerically using Eq. (8) with the theoretical estimate $(a/c)^{1/3}$. Good agreement is seen. The bottom value decreases with the peak value of the pulse, which is approximated as $2c$. These features are already found in Fig. 6.

The competitive interaction of the neighboring pulses is similar to the Ostwald ripening in the time evolution of the spinodal decomposition in two or three dimensions. The diffusion process transports mass from small droplets to large droplets in the Ostwald ripening [12]. The larger droplets grow and the smaller droplets become even smaller and disappear. In our model, the larger pulses have smaller bottom values than the smaller pulses. Mass flow in Eq. (7) is expressed as

$$J=\frac{\partial}{\partial x}\left(l+\frac{a}{l^3}+D\frac{\partial^2 l}{\partial x^2}\right)\sim\left(1-\frac{3a}{l^4}\right)\frac{\partial l}{\partial x}\sim-\frac{3a}{l^4}\frac{\partial l}{\partial x}, \quad (9)$$

where only the long intervals are considered, and l and $\partial^2 l/\partial x^2$ are assumed to be sufficiently small. Equation (7) is rewritten as a form of mass conservation using the current as

$$\frac{\partial l}{\partial t}=-\frac{\partial J}{\partial x}.$$

The slope $\partial l/\partial x$ in the long interval between the jth pulse and the $(j+1)$th pulse is evaluated as $\{(a/c_{i+1})^{1/3}-(a/c_i)^{1/3}\}/(x_{j+1}-x_j)$, where c_j and x_j are the c value and the position of the jth pulse, respectively. If the pulse height of jth pulse is larger than that of $(j+1)$th pulse, c_j is larger than c_{j+1}, then the mass current flows from the $(j+1)$th to jth pulse. Then, the jth pulse grows even more. If the pulse form is approximated at $l(x)\sim c+c\,\sin x$, the area of the pulse is approximated at $\int_{-\pi/2}^{3\pi/2} l(x)dx=2\pi c$. The area of the jth pulse increases by the current from the $(j+1)$th pulse and $(j-1)$th pulse. Therefore, the time evolution of the c value of the jth pulse is evaluated as

$$2\pi\frac{dc_j}{dt}=\frac{3a(2^4)}{\{(a/c_j)^{1/3}+(a/c_{j-1})^{1/3}\}^4}\frac{(a/c_{j-1})^{1/3}-(a/c_j)^{1/3}}{x_j-x_{j-1}}+\frac{3a(2^4)}{\{(a/c_j)^{1/3}+(a/c_{j+1})^{1/3}\}^4}\times\frac{(a/c_{j+1})^{1/3}-(a/c_j)^{1/3}}{x_{j+1}-x_j}. \quad (10)$$

This equation describes the competition of neighboring pulses. Figure 8 displays the time evolutions of three pulse heights. Figure 8(a) is an initial profile of $l(x)$ including three pulses with peak height 5.23, 6.90, and 5.42 at $x_1=27.3$,$x_2=54.3$, and $x_3=98$ in a system of $L=100$. The three solid curves display the time evolutions by Eq. (7), and the dashed curves display the time evolution by Eq. (10). [The peak amplitude is evaluated at $2c_j$ for the time evolution of Eq. (10).] Only the pulse peak of the largest pulse increases. The time evolution by Eq. (10) is a good approxi-

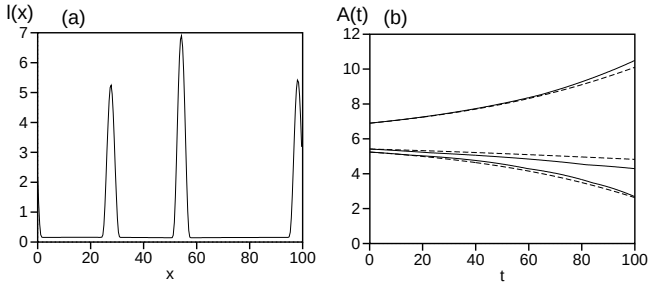

FIG. 8. Comparison of time evolutions of peak heights of three pulses by Eq. (7) (solid curves) with by Eq. (10) (dashed curves).

mation to the competitive dynamics. In the time evolution of Eq. (10), the peak amplitude at $x=x_1\sim 5.23$ decreased to zero near $t\sim 150$. One of the three pulses decays to zero and the description by Eq. (10) for the three pulses becomes meaningless.

The linear growth law of the average pulse height is also explained using this equation. If the time evolution of pulse number is expressed as $n(t)$, the interval $x_{j+1}-x_j$ is evaluated as $L/n(t)$. The c value is evaluated as $c(t)\propto L/n(t)$ from the conservation law of the total area $2\pi c(t)\times n(t)$ of pulses. Then, the time evolution of c is evaluated as $dc/dt \sim [a/c(t)]^{-4/3}\times[a/c(t)]^{1/3}/n(t)^{-1}\sim[1/c(t)]^{-1}/c(t)\sim$ const. Therefore $c(t)\sim t$, and it means that the average pulse height grows in proportional to t. This growth law is shown in Fig. 6(b) by direct numerical simulation.

IV. SUMMARY

We have proposed a discrete and a continuum model for hierarchical bunching. Long-range attractive and repulsive forces induce the bunching instability. The short-range repulsive force determines the small spacing inside the bunched clusters. Our model is a variational one, since it has a potential function, therefore the bunching process is simpler. In the models of traffic congestion and the step bunching in the crystal growth, nonvariational effects need to be considered. The nonvariational effects make the problems more complicated.

We have investigated the time evolution of the average distance between bunched clusters and found that the average distance increases with a power law for the long-rage forces. We have checked that the variance of the distance between the bunched clusters also obeys a power law with the same exponent. It is important as a next problem to study the time evolution of the distribution of the distances between the bunched clusters and the distribution of the final coalescence time to understand the dynamics of the hierarchical bunching more in detail.

The continuum model takes a similar form to a model of the spinodal decomposition. The competitive dynamics between the pulses is similar to the Ostwald ripening for the spinodal decomposition, but it is rather different from the behaviors of the Ginzburg-Landau equation for the conserved order parameter, which have been intensively studied. The competitive dynamics is an elemental process to understand the time evolution of the distribution of the distances between the bunched clusters using an equation such as the Smoluchowski equation.

[1] J.B. Gunn, Solid State Commun. **1**, 88 (1963).
[2] K. Nagel and M. Schreckenberg, J. Phys. I **2**, 2221 (1992).
[3] D. Chowdhury, L. Santen, and A. Schasschneider, Phys. Rep. **329**, 199 (2000).
[4] A.V. Latyshev, A.L. Aseev, A.B. Krasilnikov, and S.I. Stenin, Surf. Sci. **213**, 157 (1989).
[5] S. Stoyanov, Jpn. J. Appl. Phys., Part 1 **30**, 1 (1991).
[6] Y.N. Yang, E.S. Fu, and E.D. Williams, Surf. Sci. **356**, 101 (1996).
[7] M. Sato and M. Uwaha, J. Phys. Soc. Jpn. **67**, 3675 (1998).
[8] F. Gillet, Z. Csahok, and C. Misbah, Phys. Rev. B **63**, 241401 (2001).
[9] M. Bando, K. Hasebe, A. Nakayama, A. Shibata, and Y. Sugiyama, Phys. Rev. E **51**, 1035 (1995).
[10] E.g., M. Sato and M. Uwaha, J. Phys. Soc. Jpn. **65**, 1515 (1996).
[11] J.D. Gunton, M. San Miguel, and P.S. Sahni, in *Phase Transitions and Critical Phenomena*, edited by C. Domb and J.L. Lebowitz (Academic Press, New York, 1983), Vol. 8.
[12] I.M. Lifshitz and V.V. Slyozov, J. Phys. Chem. Solids **19**, 35 (1961).